Chemosphere 303 (2022) 134916

Contents lists available at ScienceDirect

Chemosphere

journal homepage: www.elsevier.com/locate/chemosphere

Evaluation of a novel integrated membrane biological aerated filter for water reclamation: A practical experience

Ali Nikoonahad [a], Abdolmajid Gholizadeh [b,*], Mohammad Taghi Ghaneian [c], Ali Paseban [d], Nayera Naimi [d,e], Mahdi Ghorbanian [d], Mahmoud Taghavi [f], Amir Mohammadi [g], Ali Abdolahnejad [g], Bagher Moradi [h]

[a] *Department of Environmental Health Engineering, School of Public Health, Ilam University of Medical Sciences, Ilam, Iran*
[b] *Department of Environmental Health Engineering, Torbat Heydariyeh University of Medical Sciences, Torbat Heydariyeh, Iran*
[c] *Environmental Science and Technology Research Center, Department of Environmental Health Engineering, School of Public Health, Shahid Sadoughi University of Medical Sciences, Yazd, Iran*
[d] *Department of Environmental Health Engineering, School of Public Health, North Khorasan University of Medical Sciences, Bojnurd, Iran*
[e] *Student Research Committee, Department of Environmental Health Engineering, School of Health, Mashhad University of Medical Sciences, Mashhad, Iran*
[f] *Department of Environmental Health Engineering, School of Public Health, Social Development & Health Promotion Research Center, Gonabad University of Medical Sciences, Gonabad, Iran*
[g] *Department of Environmental Health Engineering, Maragheh University of Medical Sciences, Maragheh, Iran*
[h] *Esfarayen Faculty of Medical Science, Esfarayen, Iran*

HIGHLIGHTS

- Employing IMBAF generated high quality feed water for membrane systems.
- IMBAF reduced sludge production, guaranteed water reuse with high quality.
- After 75 days of continuous operation, TMP increased about 14% indicating low membrane clogging.
- 99.88% of the influent was recycled, and only 0.12% was disposed as sludge.

GRAPHICAL ABSTRACT

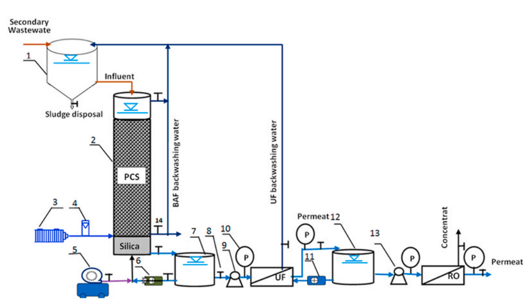

ARTICLE INFO

Handling editor: Derek Muir

Keywords:
Integrated membrane biological aerated filter (IMBAF)
Biological aerated filter (BAF)
Water reclamation
Reverse osmosis (RO)
Wastewater recycling

ABSTRACT

The use of treated wastewater in addition to solving the problem of water shortage, can increase soil fertility and reduce the use of chemical fertilizers. We aim to provide a high-quality effluent to feed membrane system, reduce treatment costs and enhance the efficiency of wastewater recycling. All experiments were conducted on a novel integrated membrane biological aerated filter (IMBAF) consisting of a down flow cylindrical biological aerated filter (BAF) filled by silica and a novel sand-coated polystyrene granules (SCP), followed by ultrafiltration (UF) and reverse osmosis (RO) membranes. IMBAF reactor, with 73.6 L volume, was operated for 270 days (in three 90-day stages) with different conditions of returning backwash water. Accordingly, BAF generated high quality water for feeding UF membrane with 94.2%, 68%, 54.4%, 91.2%, and 99.95% of turbidity, 5-day biochemical oxygen demand (BOD_5), chemical oxygen demand (COD), oil and grease (O&G), fecal coliform (FC) removal,

* Corresponding author.
E-mail address: gholizadeh_eng@yahoo.com (A. Gholizadeh).

https://doi.org/10.1016/j.chemosphere.2022.134916
Received 10 June 2021; Received in revised form 7 March 2022; Accepted 7 May 2022
Available online 18 May 2022
0045-6535/

respectively. At the end of stage 3, 99.88% of influent was recycled by UF and only 0.12% was disposed of as sludge. The BAF and UF module efficiently promote the quality of water entering RO system. After 75 days of continuous operation, the increase in *trans*-membrane pressure (TMP) and also decrease in RO membrane permeability were about 14% and 9.4%, respectively, indicating low clogging of the membrane. The use of BAF structure designed in this study increases the wastewater recycling rate, decreases membrane clogging and thereby reduces the costs of concentrate disposal and chemical cleaning.

1. Introduction

Climate change, population growth, pollution of water resources, and reduction of water resources have led people to use new advanced technologies for wastewater treatment and reuse (Yao et al., 2021). Conventional biological treatment methods cannot efficiently remove all contaminants, especially refractory impurities, pathogens, color, turbidity, and toxins (Sun et al., 2015; Zielińska et al., 2016; Salehi et al., 2020), while the regulatory standards set for purifying and reusing wastewater have become more stringent (Sagle and Freeman, 2004; Mahvi et al., 2008).

New technologies have also developed existing systems for water reclamation or wastewater reuse. Membrane-based systems, including reverse osmosis (RO), nanofiltration (NF), ultrafiltration (UF), and microfiltration (MF), often used in series, can meet our goals (Huang et al., 2020b; Yao et al., 2021). Based on earlier studies, UF can remove contaminants such as total suspended solids (TSS), bacteria, and algae, as well as some soluble macromolecules like proteins and oil and grease (O&G) (Falsanisi et al., 2010; Naghizadeh et al., 2011; Yabalak et al., 2021).

Although membrane-based systems have been rapidly developed in recent years for wastewater reclamation, they have shown some drawbacks such as fouling, membrane damage, need for chemical cleaning, and RO concentrate disposal (Oron et al., 2008; He et al., 2013; Qu et al., 2013).

Membrane units, especially RO, produce a large amount of concentrated water, which is commonly discharged into adjacent water bodies, and pose a potential threat to aquatic environments (Chen et al., 2020; Leaper et al., 2021). Almost all concentrate purification techniques such as deep well injection, evaporation ponds, electrodialysis desalination, and zero liquid discharge systems are limited in application and very expensive in operation (He et al., 2013; Gholizadeh et al., 2018; Qin et al., 2022).

Despite the increasing advances in the use of membrane technologies, research and experiences in water reclamation demonstrate that membrane fouling and damage are major challenges in the successful application of membrane-based processes (Xu et al., 2010). Suspended and dissolved solids, colloids, algae, and O&G are the major membrane fouling factors, reducing membrane lifetime, permeability, and flux (Sánchez et al., 2010; Barello et al., 2014; Gholizadeh et al., 2017). Moreover, fouling increases *trans*-membrane pressure (TMP) and finally, reduces the treatment process performance (Hasan et al., 2012; Hou et al., 2021). Wu et al. (2014) reported that among all fouling agents, colloids were of great importance (Wu et al., 2014). A review analysis conducted on fifty field studies revealed that the main parameters leading to different kinds of fouling mechanisms were related to turbidity and organic materials, especially O&G (ranged from 15 to 303 mg L^{-1}) and total organic carbon (TOC, ranged from 6.9 to 540 mg L^{-1}) (Alzahrani and Mohammad, 2014). Appropriate pretreatment conditions prolong membrane lifetime and reduce the backwash frequencies by improving the quality of membrane feed stream (Qi et al., 2011).

This study was designed to evaluate the effectiveness of a novel integrated technology (IMBAF), including an enhanced biological aerated filter (BAF) followed by UF and RO membranes. BAF, as a promising wastewater treatment technology due to limited land use and increased treatment efficiency, has a bed of filter medium providing a high surface to grow biomass on it, while the wastewater was pumped up or down through the filter (Neshat et al., 2019; Manikandan et al., 2022; Xu et al., 2022).

Here, a new media was used to improve the porosity, thereby increasing the biofilm formation, and reducing TMP of subsequent membranes. Also, for further treatment, BAF and UF effluents were returned to the beginning of the process. The objectives of this study were: 1) apply a BAF structure to increase the water reclamation efficiency and enhance the removal of pollutants to provide a suitable pretreatment for membrane systems; 2) improve membrane systems efficiency with emphasis on maximum performance in the generation of purified water; 3) reduce chemical cleaning periods; 4) solve the problem of RO concentrate disposal, and 5) diminish sludge.

2. Materials and methods

2.1. Pilot plant configuration

All experiments were conducted on a reactor consisting of a cylindrical down-flow BAF and two series-mounted membranes as illustrated in Fig. 1, based on the following descriptions:

The BAF reactor was made of polyethylene whose volume was 73.6 L (25 cm in diameter). It was filled with 20 cm of silica particles with a uniformity coefficient of 1.5 and an effective size of 0.25 mm at the bottom. Later, 130 cm of novel media, sand-coated polystyrene granules (SCP), with a particle size of about 2.5 mm (described in section 2.2) was added at the top. A free space of about 30 cm was considered to deal with the increased volume of content caused by backwashing.

The reactor diameter was selected to be about 100 times larger than media size to reduce the wall effect on BAF system performance (Moore et al., 2001; Nikoonahad et al., 2017). A stainless-steel net with a mesh diameter of 0.1 mm was placed between the silica and SCP layers to separate them. Micro-bubble air diffusers (Aqua AP-320, England) were embedded above the net. An air compressor and a water pump (Etatron, Italy) were also applied for the air and water backwashing processes, respectively. The air flow rate was controlled using a flow meter.

During operation, the backwashing process was repeated every 16–19 days based on the hydraulic head loss in the reactor (15% increase in membrane TMP). Whole BAF and UF backwashing effluents were returned to the influent tank in stages 2 and 3 through two pipes (Fig. 1) in order to decrease disposal sludge, increase water reuse, and create further opportunities for decomposition of pollutants. Thus, the excess sludge of IMBAF was expelled only via a valve embedded in the influent reservoir tank. UF and RO membranes were installed in series after the BAF reactor.

The hollow-fibre UF membrane used in this study (A726, FilmTec™, DuPont) is made of polypropylene with a pore size of about 0.02 μm, membrane area of 0.67 m^2 and a filtration mode from outside to inside. Moreover, the spiral wound RO membrane made of a polyamide thin-film (TW30-1812-100HR, FilmTec™, DuPont) with an effective area of 0.445 m^2 was employed in the reactor. Additional specifications of UF and RO membranes are summarized in Table 1. The permeate production time for UF membranes was 5 h, followed by a 2-min backwashing period. Although the TMP variations were very slight, the mentioned production time of the clean permeated water was considered to prevent the deposition and damage of UF membrane. These times were chosen based on the results of similar studies (Falsanisi et al., 2010; Qi et al., 2011).

Inlet and outlet pressures of RO and UF membranes were measured through pressure gauges mounted on the inlet and outlet of the membrane module, respectively. TMP was calculated twice a week as (Sun et al., 2015):

TMP = (inlet pressure + outlet pressure) / 2.

In addition, clean water with a turbidity of about 0.2 nephelometric turbidity unit (NTU), supplied from UF permeate reservoir tank, was used to backwash UF membrane.

2.2. *Media preparation*

To produce SCP media, a cylindrical steel container was filled with dry washed sand with a diameter of about 0.3 mm. The cylinder was heated up to about 200 °C while it was spinning. Later, polystyrene crystal granules (HIPS7240, Tabriz Petrochemical, Iran) with a range size of 2–2.5 mm were added to the container. Heating was continued

Table 1
Specifications of UF and RO membranes.

characteristic	Unit	RO	UF
Membrane type	–	Spiral	Hollow fiber
Model	–	TW30-1812-100HR	PP A-726
Material	–	polyamide thin film	Polypropylene
Total membrane area	m^2	0.445	0.67
Nominal pore size	μm	0.001–0.0001	0.02
Wastewater designed flux	$L\ min^{-1}$	0.262	1
Max-feed turbidity	NTU	5	50
Least molecular weight cut-off removable	Dalton	–	10000
Max- TMP	psi	150	30

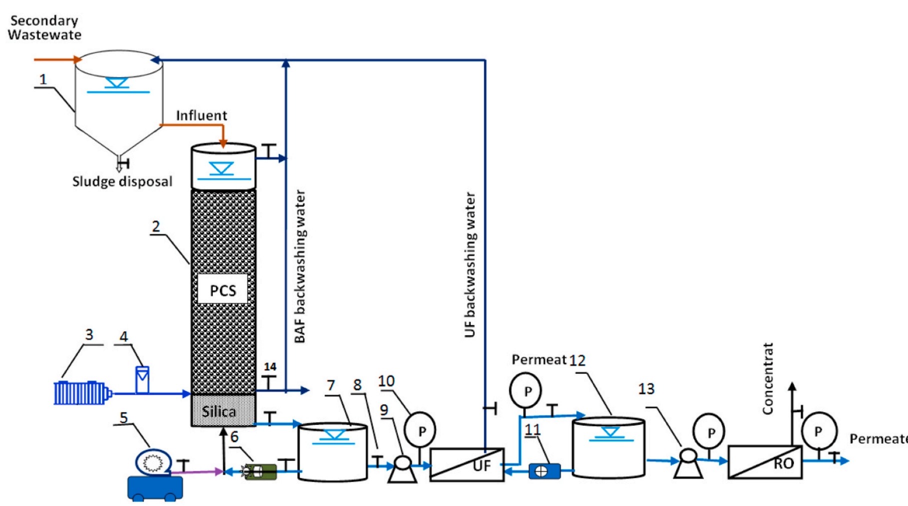

A

B

Fig. 1. A) Schematic diagram of IMBAF: (1) Influent reservoir tank; (2) BAF; (3) Air diffuser; (4) Air flow meter; (5) Air compressor; (6) Backwashing water pump; (7) reservoir of BAF effluent; (8) valve; (9) UF pressure pump; (10) Pressure gauge; (11) UF backwashing pump; (12) UF permeate reservoir; (13) RO pressure pump, and B) the actual picture.

until the polystyrene granules reached the annealing point, and sand penetrated the outer surface of them. Rotation of the cylinder was continued at the ambient temperature for 10 min until it was cool, and a uniformly rounded SCP media was formed. Therefore, the outlying surface of polystyrene granules was completely covered with sand particles. Based on the following formulas (Wu et al., 2015), SCP grain density, water absorption, and total porosity were about 730 mg L^{-1}, 1.5%, and 53%, respectively:

$$\text{Grain density } (\text{kg m}^{-3}) = \frac{\text{mass of SCP grains}}{\text{volume of SCP grains}} \quad (1)$$

$$\text{Water absorption } (\%) = \frac{\text{1 h saturated mass of SCP grains} - \text{mass of dry SCP grains}}{\text{mass of dry SCP bodies}} \times 100 \quad (2)$$

$$\text{Porosity } (\%) = \frac{\text{volume of Saturated water between the grains}}{\text{volume of SCP grains}} \times 100 \quad (3)$$

2.3. Feed water characteristics

The pilot plant was run on the effluent of municipal wastewater treatment plant (MWWTP) of Yazd, Iran. This MWWTP treats not only the municipal wastewater but also the effluents of some industrial plants. The feed flow rate of the pilot plant was 950 L d^{-1} throughout the study, which was continuously entering the pilot. The quality characteristics of influent entering the pilot have been described in Table 2, which is still not suitable for reuse.

2.4. Experimental procedures

During the BAF start-up period, approximately 10 g of milk powder, 100 mL of aerated digestion sludge, and 100 g of the wall sludge of intermittent cycle extended aeration system (ICEAS) were used daily for developing biological growth for four weeks until it reached a steady-state condition. Subsequently, the main experiments started for 270 days. The operation was divided into three different stages; Stage 1 lasted from day 1–90 and included operation without recycling backwash water. At this point, clean water and the water from backwashing BAF were discharged. Stage 2 lasted from day 91–180, in which the water from the backwash was recycled. Besides, the effect of BAF backwashing effluent on reactor performance was evaluated by returning backwashing effluent to the influent tank. Stage 3 lasted from day 181–270, during which both backwash water from BAF and UF were purified and recycled. In this stage, membrane systems were installed next to the BAF reactor.

Furthermore, the effect of simultaneous return of BAF and UF backwash effluents was investigated on BAF reactor efficiency and sludge reduction. Considering previous studies (Pramanik et al., 2012; Wang et al., 2015; Zielińska et al., 2016), the amounts of organic loading rate (OLR), hydraulic loading rate (HLR), hydraulic retention time (HRT), and water flowrate were considered at 0.74 kg m^{-3} d^{-1}, 13 m^3 m^{-3} d^{-1}, 60 min, and 0.224 L m^{-2} s^{-1}, respectively.

In some literature (WU SQ et al., 2011; Feng et al., 2013; Zhang et al., 2014), air to water ratio (A/W) value was considered as 3–15 in secondary and advanced wastewater treatments. Given that the influent OLR rate was low in this study, the A/W value was considered as 4, thereby the average concentration of dissolved oxygen (DO) was about 5 mg L^{-1}. The system was operated in the ambient air at a temperature range of about 15–35 °C.

Citric acid (pH ≈ 2) and sodium hydroxide (NaOH) solutions (pH ≈ 12) were utilized for the acid and alkaline backwashing of the membranes (Tang et al., 2014). The interval between each chemical backwash was determined based on the 15% increase in membrane TMP, achieved by pressure gauges.

Table 2
Characteristics of wastewater entering BAF.

Parameter	Unit	Average ± standard deviation (SD)
pH	–	7.2 ± 0.15
Temperature	°C	18 ± 2
Turbidity	NTU	19.7 ± 8
TSS	mg L^{-1}	40 ± 11
chemical oxygen demand (COD)	mg L^{-1}	57 ± 21
soluble chemical oxygen demand (SCOD)	mg L^{-1}	22.1 ± 5.3
5-day biochemical oxygen demand (BOD_5)	mg L^{-1}	21.2 ± 4
Nitrate-NO_3 ($N–NO_3$)	mg L^{-1}	4.6 ± 1.8
Total phosphorus (TP)	mg L^{-1}	2.4 ± 0.3
Color	PT-Co	67 ± 26
Fecal coliform (FC)	most probable number (MPN)/100 mL	$84 \times 10^5 \pm 12 \times 10^4$

2.5. Analytical methods

Samples were regularly collected for BOD_5, COD, SCOD, Color, O&G, TSS, and Fecal coliform (FC) tests twice a week, while the samples for TOC, TDS, Total Kjeldahl Nitrogen (TKN), and Nitrate-NO_3 ($N–NO_3$) tests were collected two times every month. Turbidity, DO, and temperature parameters were measured daily. Additionally, the gauge pressure amounts, as well as volume of permeate and concentrate, were determined twice a week to calculate TMP, flux, and permeability.

Samples were analyzed in terms of BOD_5, COD, SCOD, Color, TOC, O&G, $N–NO_3$, TKN, TSS, and FC and checked whether they are in accordance with the instructions provided by the APHA Standard Method or not. Other parameters such as DO, turbidity, conductivity, TDS, and pH were also measured using DO meter (WT/330, Yokogawa, Japan), turbidity meter (2100 N, Hach, USA), and conductivity/TDS/pH multimeter (HQ40d, Hach, USA), respectively. Membrane performances were evaluated based on TMP, flux, permeability, and scanning electron microscopy (SEM, Stereo Scan LEO, Model-400) analyses.

In order to evaluate the fluctuations of influent and effluent data of the BAF, their standard deviation (SD) was used. A low SD indicates that the data points are close to the average, while a high SD shows that the data points are spread over a wider range of values.

2.6. SEM analysis

After using the reactor for three consecutive months, uncleaned membranes were dislodged from the modules. Then, the dried UF and RO membrane samples were fractured carefully, fixed on a metal support, and coated with a thin layer of gold. Eventually, the membrane surface morphology was examined using the SEM method under vacuum conditions to observe possible damage and fouling of the membrane surface layer.

Table 3
Average[a] concentration of parameters in influent and effluent and removal efficiency in each section of IMBAF system.

Parameter	BAF			UF		RO		
	influent	effluent	efficiency (%)	Permeate	efficiency (%)	permeate	efficiency (%)	concentrate
Turbidity (NTU)	19.3 ± 4.9	1.3 ± 0.2	94.2	0.2 ± 0.05	81.8	0	100	1.8 ± 0.5
TSS (mg L^{-1})	40.4 ± 9.1	2.5 ± 0.4	94.2	0.35 ± 0.1	86	0	100	2.5 ± 0.1.1
BOD_5 (mg L^{-1})	24.4 ± 7.4	7.8 ± 1.6	68	5.8 ± 1.2	29	ND[b]	–	14 ± 3
COD (mg L^{-1})	55.9 ± 10	25.5 ± 3	54.4	19 ± 2	25	ND	–	51 ± 8
SCOD (mg L^{-1})	40 ± 8.3	22.5 ± 3.2	44	18 ± 2	18	ND	–	45 ± 8
TOC mg L^{-1})	10.8 ± 3.4	5.8 ± 1.2	46.3	4.6 ± 0.6	17	0.63 ± 0.12	95	9.8 ± 2.2
O&G (mg L^{-1})	40 ± 0.1	0.33 ± 0.1	91.2	0.15 ± 0.1	54	ND	–	0.28 ± 0.1
Fecal coliform (MPN/100 mL)	$84 \times 10^5 \pm 32 \times 10^5$	4200 ± 1800	99.95 (6.9 Log)	0	100	0	–	0
Conductivity (μs cm^{-1})	1300 ± 140	1303 ± 153	NC[c]	1215 ± 137	6	108 ± 13	96	2950 ± 240
TDS (mg L^{-1})	955 ± 109	954 ± 102	NC[c]	911 ± 98	5	61 ± 4	97	2381 ± 173
pH	7.2 ± 0.17	7.1 ± 0.12	NC[c]	7.3 ± 0.14	–	7.7 ± 0.2	–	7.6 ± 0.3
Color (Pt·Co)	67 ± 10	43 ± 5.16	35.8	28 ± 3	34	0	100	63 ± 13
TKN (mg L^{-1})	9.3 ± 3.2	2.45 ± 0.56	73	2.1 ± 0.4	14	0.23 ± 0.15	94	5.1 ± 0.92
N–NO_3 (mg L^{-1})	4.6 ± 1.4	5.6 ± 1.2	21	4.5 ± 1.1	19	0.5 ± 0.25	85	11.45 ± 1.12

[a] Average of three stages.
[b] Not detected.
[c] Not calculated: variations are certainly related to seasonal changes.

3. Results and discussions

3.1. Study of BAF performance

The BAF reactor was installed before the UF membrane to provide high-quality feed flow to the membrane filtration units and solve the RO concentrate disposal problem. Based on the data in Table 3, the quality of influent is not suitable for entering the membrane systems, while the effluent quality of BAF system has been improved to a large extent. For example, the average concentrations of some parameters in the BAF influent such as turbidity, TSS, BOD_5, COD, SCOD, and O&G were 19.3 NTU, 40.4 mg L^{-1}, 24.4 mg L^{-1}, 55.9 mg L^{-1}, 40 mg L^{-1}, and 40 mg L^{-1}, respectively. However, these values were reduced to 1.3 NTU, 2.5 mg L^{-1}, 7.8 mg L^{-1}, 25.5 mg L^{-1}, 22.5 mg L^{-1}, and 0.33 mg L^{-1} in the effluent, respectively.

Fig. 2a illustrates that the influent turbidity passing through the first, second, and third stages varies in the range of 14–25, 13–38, and 14–40 NTU, respectively. In the effluent, variation decreased greatly and the turbidity value was reduced to about 0.9–1.5 NTU for all stages. The results of Table 4 also indicate that the average values of influent turbidity of the first, second, and third stages were 18.5, 19.2, and 19.8 NTU; while they were 1.36, 1.40, and 1.43 NTU in the effluent, respectively. High turbidity and TSS removal may be attributed to bio-filtration through a medium that acts as a biological conversion of organic matter by the biomass attached to the media and by physical trapping of suspended particles (Abou-Elela et al., 2015). SD values of influent turbidity were 3.1, 5.2, and 5.9, respectively; but these were 0.22, 0.20, and 0.23 in the effluent, respectively. Based on the findings, SD values were low and very close to each other in the three-stage effluent. Low SD values indicate that the data points are close to the average, while a high SD value shows that the data points are spread out over a wider range of values.

The periodic peaks of influent turbidity in the second and third stages, which were repeated every 16–19 days, are related to the return of BAF backwashing effluent (Fig. 2a). It can be concluded from Table 4 and Fig. 2a that the return of BAF and UF backwash effluent in second and third stages did not have a significant effect on the turbidity removal efficiency of BAF system. Thus, BAF was able to remove turbidity with a high efficiency even in shock conditions. In general, the average removal efficiency of BAF was about 94% (Table 3). In addition, the turbidity value of 1.3 ± 0.2 NTU provides high quality water in the BAF effluent for UF membrane feeding. Huang et al. (2011) investigated the biodegradation of natural organic matter (NOM) in a BAF but with a different structure compared to our study for treating river water. They reported that BAF system can be very effective in removing turbidity and TSS if operated properly (Huang et al., 2011).

Fig. 2b illustrates the trend of BOD_5 fluctuations and removal efficiency in all three stages. As shown, the influent BOD_5 concentrations varied in the ranges of 19–25 mg L^{-1}, 19–43 mg L^{-1}, and 18–47 mg L^{-1} in stages 1, 2, and 3, respectively. However, fluctuations were adjusted in the effluent, and the concentration decreased to about 8–12 mg L^{-1} in all three stages. Generally, the average BOD_5 removal efficiency was around 68% in three stages (Table 3). Comparison among different stages (Table 4) indicates that the average values of influent BOD_5 during stages 1, 2, and 3 were 21.2 mg L^{-1}, 24.9 mg L^{-1}, and 26.9 mg L^{-1}, respectively. However, these values decreased to 8.91 mg L^{-1}, 9.42 mg L^{-1}, and 9.62 in the effluent, respectively.

SD values of influent BOD_5 concentration were 1.2, 7.7, and 9.9 in stages 1, 2 and 3, respectively. These values were very close to each other in three stages (i.e., 1.2, 1.8, and 1.8, respectively). Comparison of the three stages shows that the average BOD_5 concentration of influent and SD scores in the second and third stages was higher than the first one, but these values were very close in the three stages. The system could tolerate organic shocks caused by the return of BAF and UF backwashes. Therefore, the reactor performance was appropriate for the decomposition of biodegradable materials.

Fig. 2c shows the concentration of SCOD in the influent, which were 31–44 mg L^{-1}, 32–59 mg L^{-1}, and 31–66 mg L^{-1} in stages 1, 2, and 3, respectively. However, the variability of effluent SCOD concentration decreased largely to about 19–26 mg L^{-1}, 18–29 mg L^{-1}, and 18–31 mg L^{-1} for the three stages, respectively. According to Table 4, the average SCOD values in the influent for stages 1, 2, and 3 were 37.4, 40.8, and 42.4 mg L^{-1}, respectively. These rates were 22.1, 22.8, and 23.17 mg L^{-1} in the effluent, respectively. It can be observed that the SD values for the influent SCOD concentrations were 3.7, 8.2, and 11; while they were 2.22, 2.9, and 3.8 in the effluent, respectively. Therefore, the SD value related to SCOD concentrations in the influent of stages 2 and 3 was much higher than that of stage 1. In the effluent, although there is a slight difference between the SD values of SCOD in stages 1, 2 and 3, the values are very close to each other. Lack of a significant difference among SD values in different stages of BAF indicates that the system can successfully remove recalcitrant materials returned to stages 2 and 3 through BAF and UF backwashing process. In addition, the overall average removal efficiency of 44% during all stages (Table 3) shows that the BAF used in IMBAF system was able to eliminate nearly half of the recalcitrant materials, which were not removed in the secondary treatment by ICEAS.

The O&G removal efficiency during the three stages is shown in Fig. 2d. The recorded results indicate that influent O&G concentrations were 24–61, 17–60, and 22–65 mg L^{-1} in stages 1, 2, and 3, respectively.

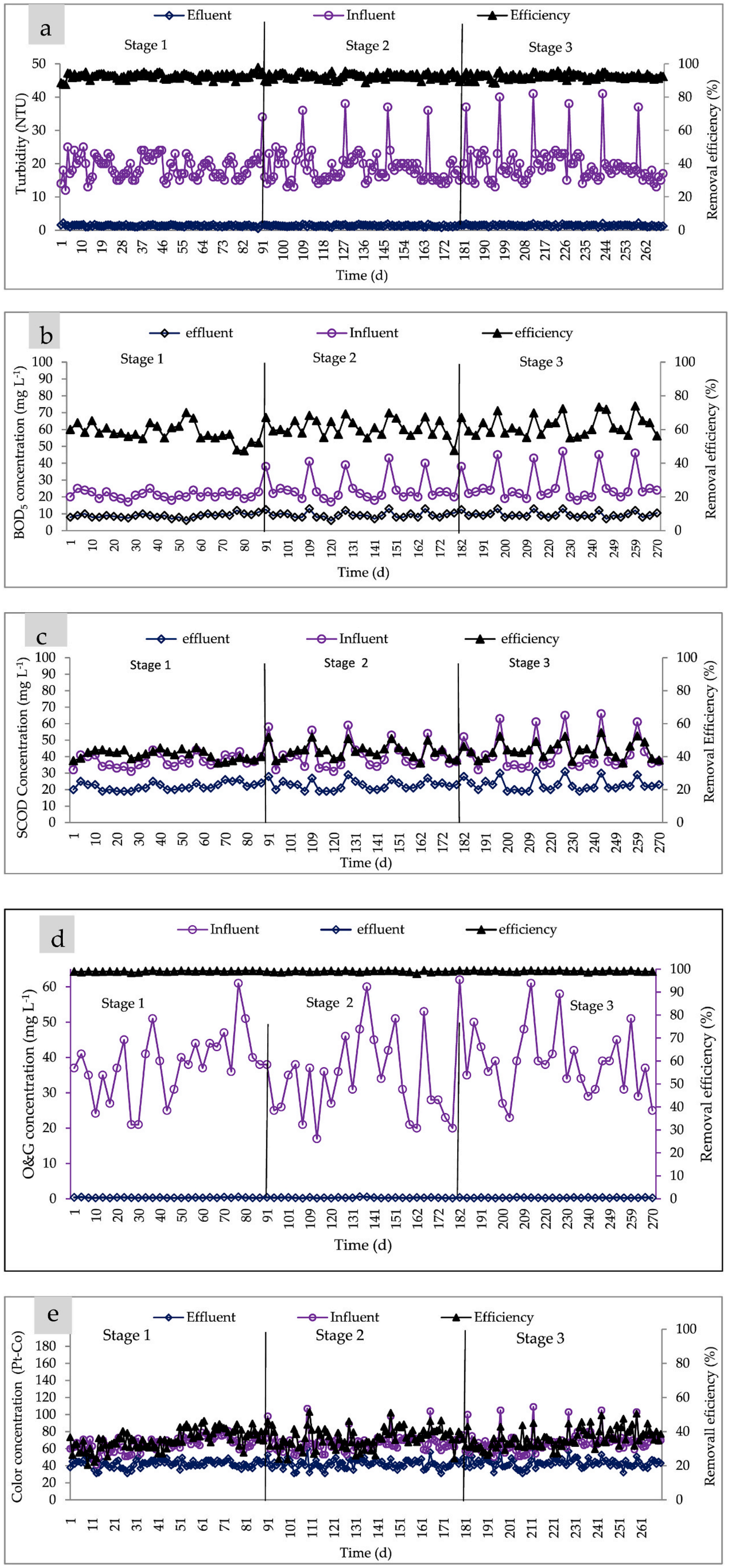

Fig. 2. The BAF time course of influent, effluent, and removal efficiency of turbidity (a), BOD_5 (b), SCOD (c), O&G (d), and color (e) during the study stages.

Table 4
Average and SD of influent and effluent pollutant concentration in different stages of BAF.

Parameters	Stages	Influent	Effluent
		Average ± SD	Average ± SD
Turbidity (NTU)	Stage 1	18.5 ± 3.1	1.36 ± 0.22
	Stage 2	19.2 ± 5.2	1.40 ± 0.20
	Stage 3	19.8 ± 5.9	1.43 ± 0.23
BOD_5 (mg L^{-1})	Stage 1	21.2 ± 2.1	8.91 ± 1.2
	Stage 2	24.9 ± 7.7	9.42 ± 1.8
	Stage 3	26.9 ± 9.5	9.62 ± 1.8
COD (mg L^{-1})	Stage 1	52.5 ± 5.3	25.44 ± 2.3
	Stage 2	56.9 ± 10.1	26.52 ± 3.0
	Stage 3	58.2 ± 13.7	26.68 ± 3.6
SCOD (mg L^{-1})	Stage 1	37.4 ± 3.7	22.1 ± 2.22
	Stage 2	40.8 ± 8.2	22.8 ± 2.9
	Stage 3	42.4 ± 11.0	23.17 ± 3.8
O&G (mg L^{-1})	Stage 1	38 ± 0.93	0.35 ± 0.07
	Stage 2	34 ± 0.11	0.31 ± 0.10
	Stage 3	40 ± 0.99	0.31 ± 0.06
Color (Pt·Co)	Stage 1	65.7 ± 7.92	42.3 ± 4.6
	Stage 2	66.9 ± 9.73	42.1 ± 5.4
	Stage 3	68.1 ± 11.52	43.3 ± 5.6

However, with a great removal efficiency of 91.2% (Tables 3 and 4), the effluent concentration reached about 0.3 mg L^{-1} after three stages. Similar investigations reported that the O&G removal rate in the BAF reactor during tertiary treatment was about 70% (Ordóñez et al., 2011; Abou-Elela et al., 2015), which is much less than the efficiency obtained in our study. Also, a similar study showed oil removal efficiencies of 54.6–80% during the treatment of synthetic oily wastewater in an aerobic batch reactor (Sanghamitra et al., 2020). In the second and third stages, some shocks were observed (Fig. 2d). However, most of them do not match with the BAF backwash time. So, these generated peaks cannot be attributed to the regular backwash process, which was performed once every 16–19 days. These fluctuations may be due to some industrial activities discharging their sewage periodically into the sewage network, or due to the cross-sectional problems in the ICEAS. The effluent O&G concentrations in tertiary treatment of similar studies were much higher than those obtained in this study. As mentioned earlier, the BAF used in this system withstood O&G shocks well. Thus, it can be concluded that the SCP rock surface layer temporarily absorbs O&G to be further degraded by biomass.

Fig. 2e and Table 4 represent that the influent color concentration in stages 1, 2, and 3 was 49–80 (average 65.7), 58–107 (average 66.9), and 61–109 (average 68.1) Pt–Co, respectively. However, these were 35–48 (average 42.3), 33–61 (average 42.1), and 34–66 (average 43.3) Pt–Co in the effluent. All peaks of color concentration that happened in the second and third stages were matched with those related to backwashing time.

SD values for influent color concentrations were 7.92, 9.73, and 11.52; while, they were 4.6, 5.4, and 5.6 for the effluent, respectively. The fact that SD values in the effluent are lower than influent in all three stages shows that BAF system can control some color shocks caused by backwashing process in stages 2 and 3. Despite the high concentration of influent color, the removal efficiency of about 43% in BAF system is considerable (Table 3). Field research indicated that such wastewater usually enters ICEAS plant from the textile industries (Al-Tohamy et al., 2022). Since the colors used in the textile industry are durable materials, the relatively low efficiency of BAF in color removal may be due to the presence of textile color (He et al., 2013; Howlader et al., 2022). It was also emphasized that biological decomposition of textile colors is difficult, because of the presence of double bond AZO groups –N=N- or double bonds of C = C, which are connected to aromatic rings in the color structure (He et al., 2013).

Table 3 shows that the removal efficiency of Fecal coliform (FC) was about 99.95% (approximately 6.9 log). Furthermore, the number of influent FC was $32 \times 10^5 \pm 4 \times 10^5$ MPN, which reached to about 4200 ± 1800 MPN in the effluent. The amount of TKN, which was about 9.3 ± 3.2 mg L^{-1} in the influent, decreased to 2.45 ± 0.56 mg L^{-1} in the effluent (approximately 73% removal).

Results of an investigation about the role of DO concentration on pollutant removal in BAF system represented that the highest decrease of TKN and NH_4–N was in a DO concentration of about 4.2 (Liu et al., 2008). The relatively appropriate removal of TKN by BAF reactor in the present study can be attributed to the suitable concentration of DO (5 mg L^{-1}). Therefore, multiple sequential shocks caused by BAF and UF backwashing did not affect the efficiency of BAF reactor. Shock tolerance and its high efficiency, especially in removing turbidity, BOD_5, SCOD, and O&G can be related to high porosity, rough surface, abundant irregular holes, relatively small size and very extensive specific surface area of the SCP media (171623 m^2 m^{-3}). Since high porosity increases HRT (Pramanik et al., 2012), rough surface reduces the velocity of pollutants and increases the contact probability of pollutant with biological agents for biodegradation as well as biofilm development (Abou-Elela et al., 2015). In addition, the smaller media size leads to better filtration to remove turbidity and TSS (Moore et al., 2001) and its unique specific surface area per volume provides large surface area for biological growth (Huang et al., 2011; Zhao et al., 2014; Abou-Elela et al., 2015).

3.2. Study of membrane performance

In stage 3, the flux, permeability, and TMP were regularly controlled to investigate the effect of BAF pretreatment on fouling phenomenon and membrane efficiency. Turbidity, O&G, and such pollutants that clog membranes and impede water passage increase TMP (Ordóñez et al., 2011). To maintain membrane safety, when the TMP of each membrane increased to about 15%, their operation was stopped, and they were chemically cleaned. Fig. 3a shows the flux, permeability, and TMP trend of UF membrane during stage 3. This figure indicates that TMP values before and after each backwash were similar from day 180–187, meaning that the membrane fouling was very low; so, the TMP value did not increase and remained approximately constant. From day 187–237, TMP levels had an increasing trend before and after each backwash. However, the amount of TMP decreased significantly after each backwash due to the removal of some blocking agents.

Although the amount of TMP decreased from day 237–255 after each backwash, the slope of TMP increment diagram after the backwash was higher than previous days (days 187–237). In other words, despite the backwash process, parts of the fouling agents, such as sticky materials, have not yet been removed from the UF membrane. The phenomenon of irreversible fouling occurs due to the presence of some organic matter such as fat, oil, gel agents due to biological growth and penetration of some turbidity factors into the depth of membrane. In such conditions, this phenomenon should be resolved by chemical washing (Sun et al., 2015). Eventually, on the 255th day, chemical washing of UF membrane caused a sharp decrease in TMP, so its value turned down again to 0.52 bar.

When TMP returned to normal, the UF permeability increased and reached the first conditions, i.e., 0.56 L m^{-2} h^{-1} bar^{-1}. From day 255 until day 270, TMP values before and after the backwashes were almost the same, and their increase was negligible. Fig. 3a shows that the increase in UF membrane TMP was only about 0.07 bar without chemical cleaning after 75 days of operation. However, in previous similar studies using UF membranes for water treatment, the TMP increased to 0.7 bar after 5 working days (Ordóñez et al., 2011), 1 bar after 14 days (Falsanisi et al., 2010), and 0.7 bar after 30 days (Wang et al., 2011). A comparison between our findings and those reported in the literature showed that the current research had better results in the backwash interval, TMP, and dependence on chemical cleaning.

These results were expected since the novel BAF system was applied as a pretreatment in this study, removing 94.2% of turbidity, 68% of

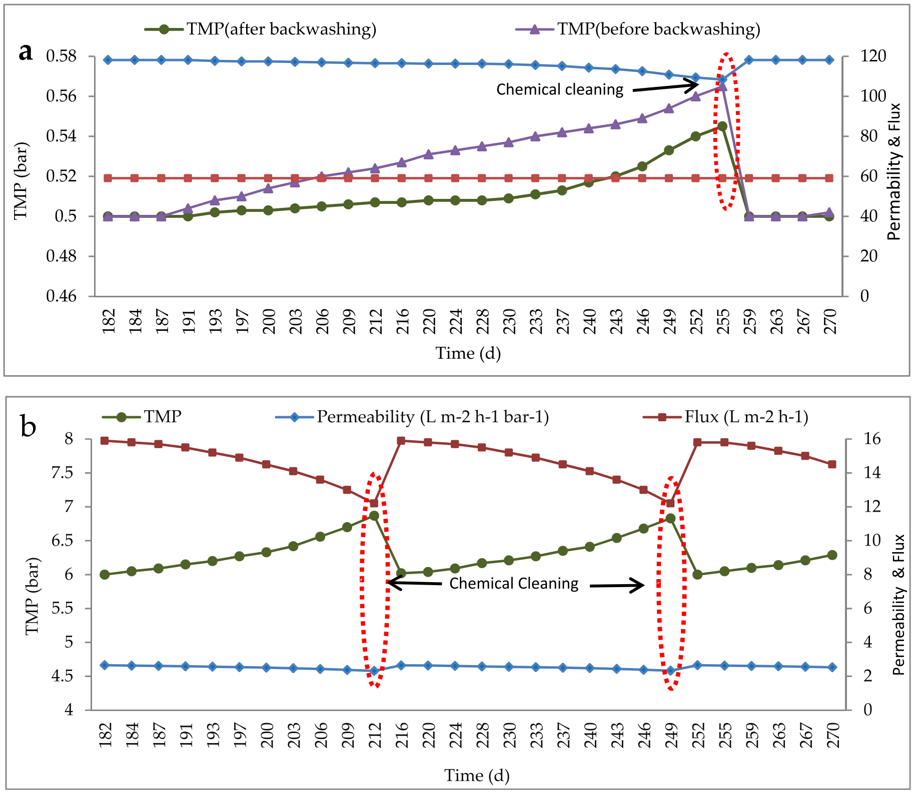

Fig. 3. Trends of TMP, flux, and permeability of UF (a) and RO (b) during operation time.

BOD_5, 54.4% of COD, 91.2% of O&G, and 99.95% of FC (Table 3), and providing very high quality water in UF membrane for feeding RO. Table 3 also indicates that the UF permeate is quite clear and the amounts of important contaminants such as turbidity, TSS, O&G, and FC, which may cause fouling in RO membrane were reduced to 81.8%, 86%, 54%, and 100%, respectively. In addition, their concentrate in UF effluent reached 0.2 ± 0.05 NTU, 0.35 ± 0.1 mg L^{-1}, 0.15 ± 0.1 mg L^{-1}, and 0 MPN, in terms of turbidity, TSS, O&G, and FC, respectively.

Fig. 3b represents the trend of flux, permeability, and TMP of RO membrane during the experiment. TMP has gradually but continuously increased at each interval between each chemical cleaning. Over a period of about a month, its value increased from 6 bar to 6.8 bar, i.e. about 15%. Similar studies reported about a 60% increase in TMP (Wang et al., 2011), which is much more than the amount obtained in our study. Therefore, the increase in TMP of only about 15% over a one-month period can be attributed to the high quality of RO feed water in the study. Comparing the quality of feed water (Table 3) with the instructions for operation and maintenance of polyamide thin-film composite used in this study (Wang et al., 2011) shows that feed water quality is much better than the instructions. Fig. 3b reveals that an increase in TMP is always associated with a relative decrease in flux and permeability. In other words, the amount of flux declines by about 24%, from 15.9 L m^{-2} h^{-1} to 12.1 L m^{-2} h^{-1} and the value of permeability by about 13.3%, from 2.65 L m^{-2} h^{-1} bar^{-1} to 2.30 L m^{-2} h^{-1} bar^{-1} in each period. However, after each chemical cleaning, the flux, permeability, and TMP returned to their original states instantly.

The effects of chemical cleaning on membrane life are not quite clear. The use of chemicals and disinfectants leads to the generation of disinfection byproducts with various health and environmental effects (Barello et al., 2014). Therefore, the use of appropriate technology in pretreatment stage decreases chemicals, energy consumption, and product disinfection, and on the other hand, increases membrane life, and finally prevents the disposal of obsolete membranes to environment as waste (Aguiar et al., 2018; Huang et al., 2020a).

3.3. Study of RO concentrate disposal

As mentioned earlier, the BAF reactor was applied in the novel IMBAF system as the pretreatment of membranes and solved the problem of RO concentrate disposal. Results of Table 4 show that the concentrations of important environmental pollutants, such as TSS, BOD_5, COD, N–NO_3, FC, and color in RO concentrate were 2.5 ± 1.1 mg L^{-1}, 14 ± 3 mg L^{-1}, 51 ± 8 mg L^{-1}, 11.42 ± 1.12 mg L^{-1}, 0 MPN/100 mL, and 63 ± 13 Pt–Co, respectively, while the standard limits of the local effluent discharge are COD $\leq$60 mg L^{-1}, $BOD_5 \leq 30$ mg L^{-1}, TSS $\leq$50 mg L^{-1}, color $\leq$75, O&G ≤ 10 mg L^{-1}, FC ≤ 400 MPN/100 mL, N–$NO_3 \leq$ 50 mg L^{-1} (Metcalf et al., 2014). Therefore, the BAF reactor used in this study not only provides a stable feed flow for high quality membrane filtration but also allows direct emission of RO concentrate in accordance with the local discharge limits of water pollutants.

The RO concentrate quality was as follows: TSS $\leq$5 mg L^{-1}, turbidity$\leq$10 NTU, FC $\leq$ 14 MPN/100 mL for irrigation of processed crops and $BOD_5 \leq$ 30 mg L^{-1}, TSS$\leq$ 30 mg L^{-1}, FC $\leq$ 200 MPN/100 mL for irrigation of the restricted landscapes. Comparison of RO concentrate quality with recommendations of environmental protection agency (EPA) shows that the RO concentration is suitable for irrigation of the processed agricultural crops and restricted landscapes. Meanwhile, the relatively high electrical conductivity (EC, 2950 ± 240 μs cm^{-1}) classifies RO concentrate as brackish water, which requires the planting of salinity-resistant plants and trees, such as pistachios and alfalfa.

3.4. SEM studies of the UF and RO membranes

To investigate the membrane morphology, the UF and RO membrane surface and pore structure were observed by SEM in Fig. 4A-D. Accordingly, the UF hollow-fibre configuration is still thoroughly intact and its surface is smooth. Furthermore, at greater magnification ratios, its pore structure is clearly visible in Fig. 4B. Due to the membrane fouling types and mechanisms developed by earlier researchers

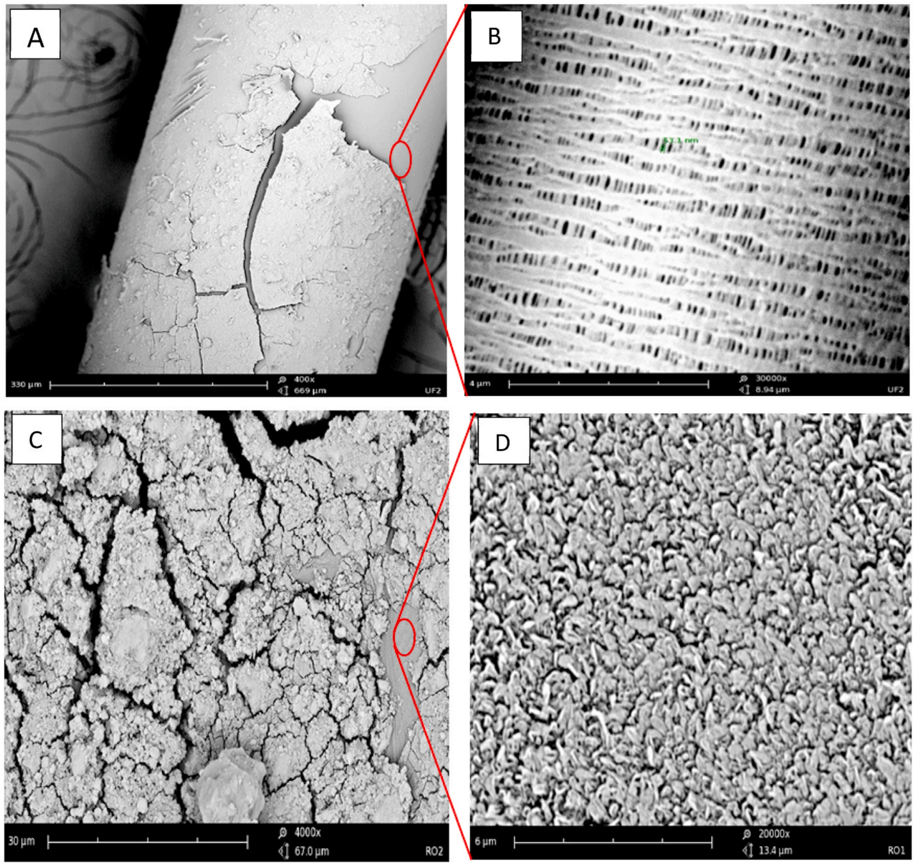

Fig. 4. SEM images of the membranes surface: (A) fouled UF, (B) structure of UF pores: (C) fouled RO, (D) structure of RO pores.

(Konsowa et al., 2013; Zuo et al., 2014), blocking pores is the primary and most important phase of fouling. However, we did not observe any UF membrane pore blockage despite three months of continuous operation (Fig. 4B). Fig. 4B also illustrates no change or damage in the pore size. Fig. 4C and D represent the fouled and porous structure of RO membrane, respectively. It can be observed clearly from Fig. 4C that the cake layer of RO membrane is cracked due to reversible deposition (Sun et al., 2015). So, it is easily removable from the membrane surface. Also, the oily contaminants are not presented in cake compositions, because they play in the deposition of oily and inorganic ions in the formation of sticky scales on the membrane surface (Zuo et al., 2014). These observations are consistent with low O&G levels in BAF effluent (Table 4). By considering Fig. 4D, the pore structure of RO membrane remains intact. It can be concluded that since the BAF system can provide a proper influent for membrane system, no membrane damage was observed and fouling was slight in the IMBAF system application.

4. Conclusions

The results of our study demonstrated that the suggested design provided high-quality physical, chemical, and biological BAF effluent to feed the membrane system. The return of BAF effluent and UF reverse membrane backwash water to the BAF reactor increased the efficiency of clean water production and removed more contaminants while causing an OLR shock. However, it had no significant effect on BAF reactor efficiency. About 99.87% of the BAF influent was recycled in the UF membrane effluent; only 0.12% of sludge was produced and excreted. After 75 days of continuous operation, the TMP of RO membrane increased by only about 14% and membrane permeability rate declined only 9.4%, indicating high efficiency of the pretreatment process. Chemical cleaning in UF membrane decreased significantly due to high removal of fouling agents by BAF reactor as a pretreatment. Accordingly, the application of IMBAF system generated feed water of high quality for membrane systems, reduced sludge production, guaranteed water reuse with high quality, and solved the problem of RO concentrate disposal.

Credit author statement

Ali Nikoonahad; study conception and design, data collection, Abdolmajid Gholizadeh; study conception and design, data collection, draft manuscript preparation, Mohammad Taghi Ghaneian; study conception and design, Ali Paseban; provide advice on study design and implementation advice, Nayera Naimi; data collection, analysis and interpretation of results, Mahdi Ghorbanian; analysis and interpretation of results, Mahmoud Taghavi; analysis and interpretation of results, Amir Mohammadi; analysis and interpretation of results, Ali Abdolahnejad; analysis and interpretation of results, draft manuscript preparation, Bagher Moradi; draft manuscript preparation. All authors reviewed the results and approved the final version of the manuscript.

Declaration of competing interest

The authors declare that they have no known competing financial interests or personal relationships that could have appeared to influence the work reported in this paper.

Acknowledgments

The authors appreciated the Shahid Sadoughi University of Medical Sciences (SSU), and all those who have cooperated in this study (project code: 4469).

References

Abou-Elela, S., Fawzy, M., El-Gendy, A., 2015. Potential of using biological aerated filter as a post treatment for municipal wastewater. Ecol. Eng. 84, 53–57.

Aguiar, A., Andrade, L., Grossi, L., Pires, W., Amaral, M., 2018. Acid mine drainage treatment by nanofiltration: a study of membrane fouling, chemical cleaning, and membrane ageing. Separ. Purif. Technol. 192, 185–195.

Al-Tohamy, R., Ali, S.S., Li, F., Okasha, K.M., Mahmoud, Y.A.-G., Elsamahy, T., Jiao, H., Fu, Y., Sun, J., 2022. A critical review on the treatment of dye-containing wastewater: ecotoxicological and health concerns of textile dyes and possible remediation approaches for environmental safety. Ecotoxicol. Environ. Saf. 231, 113160.

Alzahrani, S., Mohammad, A.W., 2014. Challenges and trends in membrane technology implementation for produced water treatment: a review. J. Water Proc. Eng. 4, 107–133.

Barello, M., Manca, D., Patel, R., Mujtaba, I.M., 2014. Neural network based correlation for estimating water permeability constant in RO desalination process under fouling. Desalination 345, 101–111.

Chen, L., Cheng, P., Ye, L., Chen, H., Xu, X., Zhu, L., 2020. Biological performance and fouling mitigation in the biochar-amended anaerobic membrane bioreactor (AnMBR) treating pharmaceutical wastewater. Bioresour. Technol. 302, 122805.

Falsanisi, D., Liberti, L., Notarnicola, M., 2010. Ultrafiltration (UF) pilot plant for municipal wastewater reuse in agriculture: impact of the operation mode on process performance. Water 2, 872–885.

Feng, Y., Qi, J., Chi, L., Wang, D., Wang, Z., Li, K., Li, X., 2013. Production of sorption functional media (SFM) from clinoptilolite tailings and its performance investigation in a biological aerated filter (BAF) reactor. J. Hazard Mater. 246, 61–69.

Gholizadeh, A., Ebrahimi, A.A., Salmani, M.H., Ehrampoush, M.H., 2017. Ozone-cathode microbial desalination cell; an innovative option to bioelectricity generation and water desalination. Chemosphere 188, 470–477.

Gholizadeh, A., Salmani, M.H., Ebrahimi, A.A., Hosseini, S.S., Ehrampoush, M.H., Miri, M., Nikoonahad, A., Pasalari, H., 2018. Improved power density and Cr/Pb removal using ozone in a microbial desalination cell. Environ. Chem. Lett. 16, 1477–1485.

Hasan, S.W., Elektorowicz, M., Oleszkiewicz, J.A., 2012. Correlations between trans-membrane pressure (TMP) and sludge properties in submerged membrane electro-bioreactor (SMEBR) and conventional membrane bioreactor (MBR). Bioresour. Technol. 120, 199–205.

He, Y., Wang, X., Xu, J., Yan, J., Ge, Q., Gu, X., Jian, L., 2013. Application of integrated ozone biological aerated filters and membrane filtration in water reuse of textile effluents. Bioresour. Technol. 133, 150–157.

Hou, B., Zhang, R., Liu, X., Li, Y., Liu, P., Lu, J., 2021. Study of membrane fouling mechanism during the phenol degradation in microbial fuel cell and membrane bioreactor coupling system. Bioresour. Technol. 338, 125504.

Howlader, M.I., Morsada, Z., Hossain, M.M., 2022. Pollutants Removal from Textile Wastewater by Biofilter. An Innovative Role of Biofiltration in Wastewater Treatment Plants (WWTPs). Elsevier, pp. 309–330.

Huang, G., Meng, F., Zheng, X., Wang, Y., Wang, Z., Liu, H., Jekel, M., 2011. Biodegradation behavior of natural organic matter (NOM) in a biological aerated filter (BAF) as a pretreatment for ultrafiltration (UF) of river water. Appl. Microbiol. Biotechnol. 90, 1795–1803.

Huang, J., Luo, J., Chen, X., Feng, S., Wan, Y., 2020a. How do chemical cleaning agents act on polyamide nanofiltration membrane and fouling layer? Ind. Eng. Chem. Res. 59, 17653–17670.

Huang, J., Zhou, Z., Zheng, Y., Sun, X., Yu, S., Zhao, X., Yang, A., Wu, C., Wang, Z., 2020b. Biological nutrient removal in the anaerobic side-stream reactor coupled membrane bioreactors for sludge reduction. Bioresour. Technol. 295, 122241.

Konsowa, A., Eloffy, M., El-Taweel, Y., 2013. Treatment of dyeing wastewater using submerged membrane bioreactor. Desalination Water Treat. 51, 1079–1090.

Leaper, S., Abdel-Karim, A., Gorgojo, P., 2021. The use of carbon nanomaterials in membrane distillation membranes: a review. Front. Chem. Sci. Eng. 1–20.

Liu, F., Zhao, C.-C., Zhao, D.-F., Liu, G.-H., 2008. Tertiary treatment of textile wastewater with combined media biological aerated filter (CMBAF) at different hydraulic loadings and dissolved oxygen concentrations. J. Hazard Mater. 160, 161–167.

Mahvi, A., Nabizadeh, R., Pishrafti, M., 2008. Evaluation of Single Stage USBF in Removal of Nitrogen and Phosphorus from Wastewater.

Manikandan, S., Subbaiya, R., Saravanan, M., Ponraj, M., Selvam, M., Pugazhendhi, A., 2022. A critical review of advanced nanotechnology and hybrid membrane based water recycling, reuse, and wastewater treatment processes. Chemosphere 289, 132867.

Metcalf, Eddy, Abu-Orf, M., Bowden, G., Burton, F.L., Pfrang, W., Stensel, H.D., Tchobanoglous, G., Tsuchihashi, R., AECOM, 2014. Wastewater Engineering: Treatment and Resource Recovery. McGraw Hill Education.

Moore, R., Quarmby, J., Stephenson, T., 2001. The effects of media size on the performance of biological aerated filters. Water Res. 35, 2514–2522.

Naghizadeh, A., Mahvi, A., Mesdaghinia, A., Alimohammadi, M., 2011. Application of MBR technology in municipal wastewater treatment. Arabian J. Sci. Eng. 36, 3–10.

Neshat, A.A., Gholizadeh, A., Jahed, B., Nikvand, P., 2019. Surveying denitrification efficacy in up-flow packed bed bioreactor operated under heterotrophic condition using autotrophic bacteria. Journal of Environmental Health and Sustainable Development 4, 851–858.

Nikoonahad, A., Ghaneian, M.T., Mahvi, A.H., Ehrampoush, M.H., Ebrahimi, A.A., Lotfi, M.H., Salamehnejad, S., 2017. Application of novel Modified Biological Aerated Filter (MBAF) as a promising post-treatment for water reuse: modification in configuration and backwashing process. J. Environ. Manag. 203, 191–199.

Ordóñez, R., Hermosilla, D., San Pío, I., Blanco, Á., 2011. Evaluation of MF and UF as pretreatments prior to RO applied to reclaim municipal wastewater for freshwater substitution in a paper mill: a practical experience. Chem. Eng. J. 166, 88–98.

Oron, G., Gillerman, L., Buriakovsky, N., Bick, A., Gargir, M., Dolan, Y., Manor, Y., Katz, L., Hagin, J., 2008. Membrane technology for advanced wastewater reclamation for sustainable agriculture production. Desalination 218, 170–180.

Pramanik, B.K., Fatihah, S., Shahrom, Z., Ahmed, E., 2012. Biological aerated filters (BAFs) for carbon and nitrogen removal: a review. J. Eng. Sci. Technol. 7, 428–446.

Qi, L., Wang, X., Xu, Q., 2011. Coupling of biological methods with membrane filtration using ozone as pre-treatment for water reuse. Desalination 270, 264–268.

Qin, L., Wang, B., Feng, P., Cao, Y., Wang, Z., Zhu, S., 2022. Treatment and resource utilization of dairy liquid digestate by nitrification of biological aerated filter coupled with assimilation of Chlorella pyrenoidosa. Environ. Sci. Pollut. Control Ser. 29, 3406–3416.

Qu, X., Alvarez, P.J., Li, Q., 2013. Applications of nanotechnology in water and wastewater treatment. Water Res. 47, 3931–3946.

Sagle, A., Freeman, B., 2004. Fundamentals of membranes for water treatment. Future Desalin. Texas 2, 137.

Salehi, H., Ebrahimi, A.A., Ehrampoush, M.H., Salmani, M.H., Fard, R.F., Jalili, M., Gholizadeh, A., 2020. Integration of photo-oxidation based on UV/Persulfate and adsorption processes for arsenic removal from aqueous solutions. Groundw. Sustain. Develop. 10, 100338.

Sánchez, A.S., Garrido, J., Méndez, R., 2010. A comparative study of tertiary membrane filtration of industrial wastewater treated in a granular and a flocculent sludge SBR. Desalination 250, 810–814.

Sanghamitra, P., Mazumder, D., Mukherjee, S., 2020. A study on aerobic biodegradation of oil and grease containing wastewater. J. Indian Chem. Soc. 97, 819–822.

Sun, X., Wang, C., Li, Y., Wang, W., Wei, J., 2015. Treatment of phenolic wastewater by combined UF and NF/RO processes. Desalination 355, 68–74.

Tang, F., Hu, H.-Y., Sun, L.-J., Wu, Q.-Y., Jiang, Y.-M., Guan, Y.-T., Huang, J.-J., 2014. Fouling of reverse osmosis membrane for municipal wastewater reclamation: autopsy results from a full-scale plant. Desalination 349, 73–79.

Wang, D., Tong, F., Aerts, P., 2011. Application of the combined ultrafiltration and reverse osmosis for refinery wastewater reuse in Sinopec Yanshan Plant. Desalination Water Treat. 25, 133–142.

Wang, H., Dong, W., Li, T., Liu, T., 2015. A modified BAF system configuring synergistic denitrification and chemical phosphorus precipitation: examination on pollutants removal and clogging development. Bioresour. Technol. 189, 44–52.

Wu, J., Contreras, A.E., Li, Q., 2014. Studying the impact of RO membrane surface functional groups on alginate fouling in seawater desalination. J. Membr. Sci. 458, 120–127.

Wu, S., Qi, Y., Yue, Q., Gao, B., Gao, Y., Fan, C., He, S., 2015. Preparation of ceramic filler from reusing sewage sludge and application in biological aerated filter for soy protein secondary wastewater treatment. J. Hazard Mater. 283, 608–616.

Wu Sq, Y., Qi Yf, G., Han, S., Yue, M., 2011. Preparation of ultra-lightweight sludge ceramics (ULSC) and application for pharmaceutical advanced wastewater treatment in a biological aerobic filter (BAF). Bioresour. Technol. 102, 2296.

Xu, H., Yang, B., Liu, Y., Song, X., Sand, W., 2022. Chapter 8 - recent advances on the treatment of domestic wastewater by biological aerated filter. In: Shah, M., Rodriguez-Couto, S., Biswas, J. (Eds.), An Innovative Role of Biofiltration in Wastewater Treatment Plants (WWTPs). Elsevier, pp. 155–170.

Xu, P., Bellona, C., Drewes, J.E., 2010. Fouling of nanofiltration and reverse osmosis membranes during municipal wastewater reclamation: membrane autopsy results from pilot-scale investigations. J. Membr. Sci. 353, 111–121.

Yabalak, E., Ozay, Y., Gizir, A.M., Dizge, N., 2021. Water recovery from textile bath wastewater using combined subcritical water oxidation and nanofiltration. J. Clean. Prod. 290, 125207.

Yao, Y., Zhang, P., Jiang, C., DuChanois, R.M., Zhang, X., Elimelech, M., 2021. High performance polyester reverse osmosis desalination membrane with chlorine resistance. Nat. Sustain. 4, 138–146.

Zhang, S., Zheng, J., Chen, Z., 2014. Combination of ozonation and biological aerated filter (BAF) for bio-treated coking wastewater. Separ. Purif. Technol. 132, 610–615.

Zhao, X.-l., Zhu, L., Bai, S.-j., Zhou, M., Qian, J., Wu, W., 2014. Performance of a double-layer BAF using zeolite and ceramic as media under ammonium shock load condition. Water Sci. Eng. 7, 81–89.

Zielińska, M., Bułkowska, K., Cydzik-Kwiatkowska, A., Bernat, K., Wojnowska-Baryła, I., 2016. Removal of bisphenol A (BPA) from biologically treated wastewater by microfiltration and nanofiltration. Int. J. Environ. Sci. Technol. 13, 2239–2248.

Zuo, X., Wang, L., He, J., Li, Z., Yu, S., 2014. SEM-EDX studies of SiO2/PVDF membranes fouling in electrodialysis of polymer-flooding produced wastewater: diatomite, APAM and crude oil. Desalination 347, 43–51.